Food Research International 109 (2018) 325–333

Contents lists available at ScienceDirect

Food Research International

journal homepage: www.elsevier.com/locate/foodres

Inactivation dynamics of 222 nm krypton-chlorine excilamp irradiation on Gram-positive and Gram-negative foodborne pathogenic bacteria

Jun-Won Kang[a,b], Sang-Soon Kim[a,b], Dong-Hyun Kang[a,b,*]

[a] Department of Food and Animal Biotechnology, Department of Agricultural Biotechnology, Center for Food and Bioconvergence, Research Institute for Agricultural and Life Sciences, Seoul National University, Seoul 08826, Republic of Korea

[b] Institutes of Green Bio Science & Technology, Seoul National University, Pyeongchang-gun, Gangwon-do 25354, Republic of Korea

ARTICLE INFO

Keywords:
Ultraviolet irradiation
Krypton-chlorine excilamp
Inactivation mechanism
Foodborne pathogenic bacteria

ABSTRACT

The object of this study was to elucidate the bactericidal mechanism of a 222 nm Krypton Chlorine (KrCl) excilamp compared with that of a 254 nm Low Pressure mercury (LP Hg) lamp. The KrCl excilamp had higher bactericidal capacity against Gram-positive pathogenic bacteria (*Staphylococcus aureus* and *L. monocytogenes*) and Gram-negative pathogenic bacteria (*S.* Typhimurium and *E. coli* O157:H7) than did the LP Hg lamp when cell suspensions in PBS were irradiated with each type of UV lamp. It was found out that the KrCl excilamp induced cell membrane damage as a form of depolarization. From the study of respiratory chain dehydrogenase activity and the lipid peroxidation assay, it was revealed that cell membrane damage was attributed to inactivation of enzymes related to generation of membrane potential and occurrence of lipid peroxidation. Direct absorption of UV radiation which led to photoreaction through formation of an excited state was one of the causes inducing cell damage. Additionally, generation of ROS and thus occurrence of secondary damage can be another cause. The LP Hg lamp only induced damage to DNA but not to other components such as lipids or proteins. This difference was derived from differences of UV radiation absorption by cellular materials.

1. Introduction

In recent years, consumers have shown increasing interest in health, resulting in increased intake of fresh or minimally processed foods (Fan, Huang, & Chen, 2017; Mir, Shah, & Mir, 2016). However, it is essential for the food industry to take appropriate measures to prevent incidence of foodborne infections due to foods contaminated with pathogens that cause foodborne disease outbreaks (Liao et al., 2017; Sivapalasingam, Friedman, Cohen, & Tauxe, 2004; Ziuzina, Patil, Cullen, Keener, & Bourke, 2014). Although heat treatment is the most commonly used sterilization technique to inactivate pathogens, conventional thermal sterilization may cause detrimental effects on sensory and nutritional characteristics of fresh food products (Berk, 2008; Gayán, Serrano, Pagán, Álvarez, & Condón, 2015). In order to maintain nutritional and sensory quality and to ensure food safety from pathogenic bacteria, non-thermal sterilization techniques can be an alternative to overcome some of the disadvantages inherent in conventional heat sterilization technique. Ultraviolet (UV) irradiation is one of several non-heat sterilization techniques that can control foodborne pathogens and has been demonstrated to effectively inactivate foodborne pathogens contaminated on food surfaces (Mikš-Krajnik et al., 2015). UV radiation has numerous advantages over conventional chemical treatment such as no disinfectant residuals, negligible formation of disinfection by-products (DBPs), no introduction of disinfectant-resistance to bacteria, and facilitation of retrofitting into existing processes (Aoyagi et al., 2011; Dotson, Rodriguez, & Linden, 2012; Lubello, Gori, Nicese, & Ferrini, 2004; Mori et al., 2007). UV disinfection systems commonly use either low-pressure (LP) or medium-pressure (MP) mercury lamps (Beck, Wright, Hargy, Larason, & Linden, 2015; Chevremont, Boudenne, Coulomb, & Farnet, 2013a). LP lamps emit monochromatic light at 253.7 nm and lesions in nucleic acid (DNA and RNA) primarily occur due to their relative peak absorbance at 260 nm. MP lamps emit polychromatic light across the electromagnetic spectrum and their broad wavelength causes not only nucleic acid damage, but also photochemical reactions in proteins and enzymes (Beck et al., 2015; Harm, 1980). Even though these lamps are widely utilized in water treatment systems, there are still many concerns about their use. The major issue is that these lamps are constructed from fragile quartz material and contain toxic mercury which is hazardous to the environment and requires proper disposal (Chevremont, Boudenne, Coulomb, & Farnet, 2013b; Close, Ip, & Lam, 2006). Moreover, these lamps have a short lifetime, a long warm-up time, and variability of radiation intensity

* Corresponding author at: Department of Agricultural Biotechnology, Seoul National University, Seoul, 08826, Republic of Korea.
E-mail address: kang7820@snu.ac.kr (D.-H. Kang).

https://doi.org/10.1016/j.foodres.2018.04.018
Received 27 November 2017; Received in revised form 2 April 2018; Accepted 12 April 2018
Available online 13 April 2018
0963-9969/

according to temperature (Chatterley & Linden, 2010; Ha, Lee, & Kang, 2017).

Dielectric barrier discharge (DBD)-driven excilamps (excimer or exciplex lamps) are regarded as an attractive alternative to conventional mercury lamps due to wavelength-selective applications, fast warm-up, absence of mercury, geometric variability, and long lifetime (Galina Matafonova & Batoev, 2012; Sosnin, 2007). This relatively new UV source is based on the transition of rare gas excited dimers, halogen excited dimers or rare gas halide excited complexes, and emit nearly monochromatic radiation at wavelengths ranging from 172 to 345 nm depending on the type of rare gas and halogen used (Galina Matafonova & Batoev, 2012; Orlowska, Koutchma, Kostrzynska, & Tang, 2015). Recently, several authors evaluated germicidal efficacy of excilamps and determined that various types (Xe_2-, KrCl-, NeXe-, and XeBr-excilamp with maximum emission at 172, 222, 270, and 282 nm, respectively) were shown to be effective in the inactivation of pathogens (Caillier et al., 2015; Clauss, Springorum, & Hartung, 2009; Ha et al., 2017; Matafonova, Batoev, Astakhova, Gomez, & Christofi, 2008; Rahmani et al., 2010; Wang, Oppenländer, El-Din, & Bolton, 2010; Yin, Zhu, Koutchma, & Gong, 2015). Yin et al. (2015) found that inactivation of *E. coli* O157:H7 with irradiation at 222 nm (KrCl) was higher than that following irradiation at 254 nm (LP Hg) or 282 nm (XeBr) in apple juice. Wang et al. (2010) reported that inactivation of *Bacillus subtilis* spores following exposure at 222 nm (KrCl) was higher than that at 254 nm (LP Hg) while inactivation after exposure at 172 nm (Xe_2) was much lower than after exposure at the other two wavelengths. Based on these previous studies, the KrCl excilamp (222 nm) potentially could an alternative to conventional mercury lamps for microorganism disinfection. However, most of the studies involving KrCl excilamps have focused on verification of disinfection efficacy. Although Ha et al. (2017) identified the inactivation mechanisms of KrCl excilamps that disrupt bacterial cell membranes and enzymatic activities, there is still need of a more quantitative, in-depth understanding of the primary pathway of disinfectant interaction with microorganisms to serve as a baseline for practical application of KrCl excilamp technology requiring further studies with KrCl excilamps. To address these issues, we compared the efficacy for inactivation of Gram-positive (*Staphylococcus aureus* and *L. monocytogenes*) and Gram-negative (*S.* Typhimurium and *E. coli* O157:H7) foodborne pathogenic bacteria, and conducted an in-depth study to ascertain the differences in inactivation mechanisms between a KrCl excilamp and a conventional LP Hg lamp.

2. Materials and methods

2.1. Bacterial cultures and cell suspension

Four strains each of *E. coli* (ATCC 35150, ATCC 43889 and ATCC 43890), *L. monocytogenes* (ATCC 19111, ATCC 19115, and ATCC 15313), *S. aureus* (ATCC 27649, ATCC 25923, and ATCC 27213), and *S.* Typhimurium (ATCC 19585, ATCC 43971, and DT 104) were provided by the bacterial culture collection of the School of Food Science, Seoul National University (Seoul, South Korea), for this study. Stock cultures were prepared by growing strains in 5 ml of tryptic soy broth (TSB; Difco, BD) at 37 °C for 24 h, combining 0.7 ml with 0.3 ml of sterile 50% glycerol and then storing at −80 °C. Working cultures were streaked onto Tryptic Soy Agar (TSA; Difco, BD), incubated at 37 °C for 24 h and stored at 4 °C for < 1 mo. Each strain of *E. coli*, *L. monocytogenes, S. aureus,* and *S.* Typhimurium was cultured in 10 ml TSB at 37 °C for 24 h, harvested by centrifugation at 4000*g* for 20 min at 4 °C and washed three times with sterile 0.2% peptone water (PW, Bacto, Sparks, MD). The final pellets were resuspended in 250 ml phosphate-buffered saline (PBS; 0.1 M) to yield approximately 10^7 to 10^8 CFU/ml.

2.2. Experimental apparatus and treatment

A DBD excilamp (29 × 9 × 8 cm; UNILAM, Ulsan, South Korea) filled with a KrCl gas mixture with output power of 20 W was used for disinfection with 222 nm UV irradiation in a bench-scale experiment. The excilamp was of cylindrical geometry covered by a metal case having a UV exit window with an area of 60 cm^2 (10 cm × 6 cm). A modulated electrical field was applied to a quartz glass body filled with KrCl gas. The quartz glass acted as a dielectric barrier and prevented the formation of plasma from short-circuiting the electrodes (inner-outer). A conventional LP Hg lamp (G10 T5/4P, 357 mm; Sankyo, Japan) with an output power of 16 W was used for a 254 nm UV irradiation bench-scale disinfection experiment. The LP Hg lamp was placed inside an aluminum reflector to focus the irradiation in one direction because LP Hg lamps radiate in all directions and the UV output window area was adjusted to fit that of the KrCl excilamp (10 cm × 6 cm). The two lamp systems were positioned vertically and directly above the samples and the vertical distance between the emitters and sample was 13 cm. Radiation intensities were measured with a UV fiber optic spectrometer (AvaSpec-ULS2048; Avantes, Eerbeek, Netherlands) calibrated to a range of 200 to 400 nm within the UV-C spectrum and the light intensities of the KrCl excilamp and LP Hg lamp were 0.29 and 0.87 mW/cm^2, respectively, at the sample location at that distance. Treatment samples were prepared by transferring 5 ml of cell suspension (described previously) into petri dishes (60 mm × 15 mm) and then treated at room temperature (21 ± 1 °C) with the 222 nm KrCl excilamp or 254 nm LP Hg lamp at equal dosages of 1, 2, 3, 4, 5, and 6 mJ/cm^2; UV doses were calculated by multiplying irradiance values by the irradiation times.

2.3. Bacterial enumeration

For enumeration of pathogens, 1 ml aliquots of treated samples were tenfold serially diluted in 9 ml of sterile 0.2% buffered peptone water and 0.1 ml aliquots of samples or diluents were spread-plated onto selective media., Sorbitol MacConkey Agar (SMAC; Difco), Oxford agar base with Bacto Oxford antimicrobial supplement (MOX; Difco), Baird Parker Agar (BPA; MB cell), and Xylose lysine desoxycholate agar (XLD; Difco) were used as selective media for the enumeration of *E. coli*, *L. monocytogenes*, *S. aureus*, and *S.* Typhimurium, respectively. All plates were incubated at 37 °C for 24 h before counting and colonies were enumerated and calculated as $\log_{10}$ CFU/ml.

2.4. Enumeration of injured cells

The overlay method was used to count injured cells of *S. aureus*, *L.monocytogenes* and *S.* Typhimurium (Lee & Kang, 2001). TSA, a nonselective medium, was used to resuscitate injured cells. One-tenth milliliter aliquots of appropriate dilutions were spread plated in duplicate, and the plates were incubated at 37 °C for 2 h to enable injured cells to recover. The resuscitated media plates were then overlaid with 7 ml of the selective medium BPA, OAB and XLD for *S. aureus*, *L. monocytogenes* or *S.* Typhimurium, respectively. The solidified plates were incubated at 37 °C for an additional 22 h. After incubation, typical black colonies characteristic of the pathogens were counted.

Enumeration of injured *E. coli* O157:H7 cells was accomplished with SPRAB (Rhee, Lee, Hillers, McCurdy, & Kang, 2003). After incubation at 37 °C for 24 h, white colonies characteristic of *E. coli* O157:H7 were enumerated, and simultaneously, serological confirmation (RIM; *E. coli* O157:H7 latex agglutination test; Remel, Lenexa, KS, USA) was performed on randomly selected presumptive *E. coli* O157:H7 colonies.

2.5. Analysis of inactivation mechanisms

Inactivation mechanisms were investigated by analyzing the DNA damage, degree of lipid peroxidation, change in cell membrane potential, intracellular enzyme activity, and generation of reactive oxygen species (ROS) during each disinfection process. For these analyses, *E. coli* O157:H7, *Listeria monocytogenes*, *Salmonella Typhimurium*, and

Staphylococcus aureus cells were adjusted to an optical density at 600 nm (OD_{600}) of approximately 0.3 in PBS and then treated to the same level of inactivation (5 log reduction).

2.5.1. Modeling of survival curves

For adjusting each treatment to the same level of inactivation (5 log reduction), D_{5d}, which indicates dosage necessary for achieving 5 log reduction, for each treatment was calculated using modeling equations.

Survival curves were fitted with the Weibull models by using GInaFiT (Geeraerd, Valdramidis, & Van Impe, 2005). The parameters of the Weibull model (δ and p) were calculated from the following equation (van Boekel, 2002):

$$\log(N) = \log(N_0) - \left(\frac{t}{\delta}\right)^p$$

where N (CFU/ml) is the population of the microorganisms, N_0 is the initial population, t (minutes) is the treatment time, δ (minutes) is the time for the first decimal reduction, and p is the parameter related to shape of the line, such as a concave downward survival curve when $p > 1$ and a concave upward curve when $p < 1$.

2.5.2. Membrane potential assay

Cell membrane potential was assessed with a membrane potential sensitive probe $DiBAC_4(3)$ (Kramer & Muranyi, 2014). This fluorescent dye accumulates in depolarized cells, but is excluded from the inner membrane when cells can maintain a transmembrane potential gradient. So, the degree of depolarization of cell membranes can be evaluated by the fluorescence value of the dye accumulated inside cells.

Suspensions of *S. aureus* and *L. monocytogenes* were incubated with 0.5 μg/ml bis-(1,3-dibutylbarbituric acid) trimethine oxonol [$DiBAC_4(3)$; Molecular Probes, Invitrogen, Thermo Fisher Scientific; Waltham, MA, USA] at room temperature for 2 min in the dark. Suspensions of *E. coli* O157:H7 and *S.* Typhimurium were incubated with 2.5 μg/ml $DiBAC_4(3)$ with 4 mM ethylenediaminetetraacetic acid (EDTA) at 37 °C for 15 min in the dark. After incubation, each dyed sample was centrifuged at 10,000 × *g* for 10 min and washed twice with PBS to remove excess dye. The cell pellet was resuspended in PBS, and fluorescence was measured with a Spectramax M2e at excitation and emission wavelengths of 488 and 525 nm, respectively.

2.5.3. Detection of the end products of lipid peroxidation

Lipid peroxidation, a type of unstable oxidative stress in plant, animal and microbial cells, leads to decomposition resulting in the formation of quite complex and reactive compounds such as malon dialdehyde (MDA) and 4-hydroxynonenal (4-HNE). The occurrence of MDA was detected using thiobarbituric acid (TBA) which forms the MDA-TBA adduct and the degree of lipid peroxidation was measured by the fluorescence intensity of the MDA-TBA adduct. The thiobarbituric acid reactive substance (TBARS) assay is a well-established assay for monitoring lipid peroxidation (Joshi et al., 2011). The quantity of malonaldehyde (MDA) was analyzed using the OxiSelect TBARS Assay Kit (Cell BioLabs, Inc., San Diego, CA), following the manufacturer's directions. One milliliter of treated sample was centrifuged at 10,000*g* for 10 min and the supernatant was discarded and the pellet resuspended in PBS containing 1× Butylated hydroxytoluene (BHT). Each sample was mixed with 100 μl SDS lysis solution and incubated at room temperature for 5 min. Following incubation, each sample was reacted with 250 μl of TBA reagent at 95 °C for 1 h and thereafter cooled to room temperature in an ice bath for 5 min. Samples were centrifuged at 3000 RPM for 15 min and then fluorescence of the supernatant was measured with a Spectramax M2e at excitation and emission wavelengths of 540 and 590 nm, respectively.

2.5.4. Detection of intracellular ROS

$CM\text{-}H_2DCFDA$ is a cellular assay probe used for the detection of intracellular ROS. This probe can freely penetrate the cell membrane and be hydrolyzed in the cell to form the dichlorofluorescin (DCFH) carboxylate anion and then converted to highly fluorescent 2′,7′-dichlorofluorescein (DCF) upon oxidation by ROS (Kalyanaraman et al., 2012; Negre-Salvayre et al., 2002; Wojtala et al., 2014). Therefore, the extent of generation of intracellular ROS was determined from increasing fluorescence values of DCF.

Treated samples were incubated with $CM\text{-}H_2DCFDA$ [5-(and-6)-chloromethyl-2′,7′ -dichlorodihydrofluorescein diacetate, Invitrogen] at a final concentration of 5 μM for 15 min at 37 °C. After incubation, cells were collected by centrifugation at 10,000 × *g* for 10 min and washed twice with PBS and fluorescence measured with a spectrofluorophotometer at excitation and emission wavelengths of 495 and 520 nm, respectively.

2.5.5. DNA damage assay

SYBR green I [2-[*N*-(3-dimethylaminopropyl)-*N*-propylamino]-4-[2,3-dihydro-3-methyl-(benzo-1,3-thiazol-2-yl)-methylidene]-1-phenylquinolinium] was used to examine DNA damage (Han et al., 2016). SYBR green I has an ability to dramatically (> 1000-fold) increase brightness upon interaction with double-strand DNA (dsDNA) and thus can be used to quantify nucleic acid (Dragan et al., 2012). Therefore, it was used an indicator of DNA damage because the fluorescence signal of SYBR green I would decrease in the event of DNA damage.

Following treatment, *E. coli* O157:H7 and *Salmonella* Typhimurium samples were incubated with 100 μg/ml lysozyme (which hydrolyzes the bacterial cell wall by breaking 1–4 bonds between *N*-acetyl-β-D-glucosamine (NAG) and *N*-acetyl-β-D-muramic acid (NAM) in peptidoglycan) at 37 °C for 4 h to release the intracellular DNA. *L. monocytogenes* and *S. aureus* samples were incubated with not only 100 μg/ml lysozyme but also 10 μg/ml lysostaphin, which is capable of cleaving the polyglycine cross-links in peptidoglycan, at 37 °C for 4 h due to the different cell wall structure of Gram-positive bacteria. After incubation, SYBR green I (1:10,000 dilution; Molecular Probes, Eugene, OR, USA) at a working concentration (1:1) was applied for 15 min at 37 °C. A 200 μl aliquot of each sample was transferred to a 96-well fluorescence microplate and fluorescence was measured with a spectrofluorophotometer (Spectramax M2e; Molecular Devices, CA, USA) at excitation and emission wavelengths of 485 and 525 nm, respectively.

2.5.6. Enzymatic activity assay

The enzymatic activity of respiratory chain dehydrogenase was determined by conversion of colorless INT to water-insoluble and dark red iodonitrotetrazolium formazan (INF) by the bacterial respiratory chain dehydrogenase (Li et al., 2010); thus the loss of respiratory chain enzymatic activity can be assessed by decreasing spectrophotometric value of INF.

Following treatment, 0.9 ml of treated sample was mixed with 0.1 ml of 0.5% iodonitrotetrazolium chloride (INT) solution. After incubation at 37 °C in the dark for 2 h, cells were collected by centrifugation and dissolved in 1 ml of acetone-ethanol (1:1 ratio) mixture. Dehydrogenase activity was then assayed through formazan formation by measuring absorbance of INF at 490 nm with a Spectramax M2e.

The fluorescence or absorbance values obtained from each assay were normalized for OD_{600} to represent each of the following values: Depolarization value, The end products of lipid peroxidation value, Respiratory chain dehydrogenase activity value, Intracellular ROS generation value, and DNA integrity value.

2.6. Statistical analysis

All experiments were replicated three times. All experiments for pathogen inactivation were duplicate-plated. All data were analyzed by the ANOVA procedure of SAS (Version 9.4. SAS Institute Inc., Cary, NC, USA) and mean values of log reduction of microorganism populations or D_{5d} or fluorescence/absorbance values normalized for OD_{600} were separated using the LSD *t*-test. A probability level of $P < .05$ was used

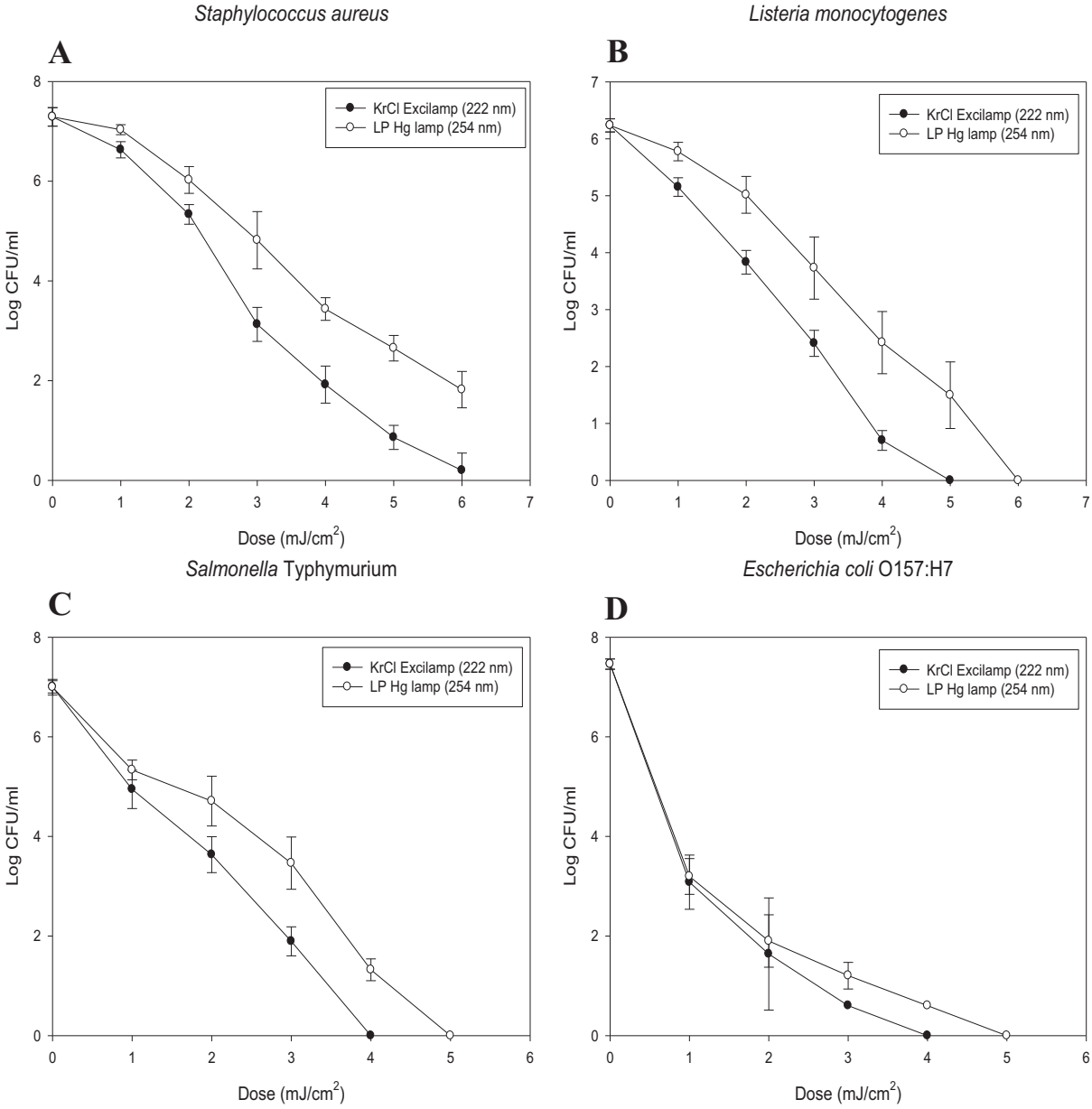

Fig. 1. Log CFU/ml populations of *Staphylococcus aureus* (A), *Listeria monocytogenes* (B), *Salmonella* Typhimurium (C), and *Escherichia coli* O157:H7 (D) suspended in PBS treated with a KrCl excilamp (222 nm) and LP Hg lamp (254 nm).
*Significant differences ($P < .05$) in microorganism populations (Log CFU/ml) occurred between the KrCl excilamp and LP Hg lamp at all treatment dosages except for 1 and 1–2 mJ/cm^2 treatment of *S.* Typhimurium and *E. coli* O157: H7, respectively.

to determine significant differences.

3. Results and discussion

Fig. 1 depicts surviving populations of *S. aureus* (A), *L. monocytogenes* (B), *S.* Typhimurium (C), and *E. coli* O157:H7 (D) resuspended in PBS after irradiation with the KrCl excilamp (222 nm) and LP Hg lamp (254 nm). From the results, the KrCl excilamp provided significantly ($P < .05$) stronger bactericidal effect of the cell suspensions in PBS compared to that of the LP Hg lamp, and *S. aureus* showed the highest resistance to UV irradiation for both lamp treatments followed by *L. monocytogenes*, *S.* Typhimurium, and *E. coli* O157:H7, respectively. The results from our study on the bactericidal effect is in accordance with previous studies conducting comparative research on the bactericidal effect between the KrCl excilamp and LP Hg lamp which revealed that the KrCl excilamp was superior to conventional Hg lamps (Ha et al., 2017; Wang et al., 2010; Yin et al., 2015). Therefore, the results from the present study support the potential utilization of KrCl excilamps as an UV alternative to conventional LP Hg lamps. For effective practical application or further studies involving KrCl excilamps, however, there **is** need to elucidate the inactivation mechanisms of the KrCl excilamp. Prior to mechanisms analysis, modeling of survival curves was conducted to calculate the D_{5d} value to analyze the inactivation mechanisms of the KrCl excilamp and LP Hg lamp at the same level of inactivation (5 log reduction). Among the various models, it was found that the Weibull model was well-fitted to the inactivation data because high R^2 (≥ 0.96) values were observed, which indicates that the regression line from the model fits well for inactivation of the pathogens. The parameters δ and S_1 in the Weibull model represent the time needed in the early stage of inactivation and these parameters were used to calculate the D_{5d} value (Table 1). Then, we conducted multiple analysis of inactivation mechanisms of the KrCl excilamp

Table 1
Parameters of the Weibull model for inactivation of *S. aureus*, *L. monocytogenes, S*. Typhimurium and *E. coli* O157:H7 treated with a LP Hg lamp and KrCl excilamp corresponding to irradiation dose (mJ/cm^2) profiles and the calculated D_{5d} values which indicate which dosages are necessary for achieving 5-log reductions using model equations.

Irradiated wavelength	Weibull			
	δ (mean ± SE)	*p* (mean ± SE)	R^2	D_{5d} (mean ± SD)
Staphylococcus aureus				
LP Hg lamp (254 nm)	1.32 ± 0.30	1.18 ± 0.21	0.98	5.23 ± 0.12 A
KrCl exilamp (222 nm)	0.74 ± 0.08	0.98 ± 0.04	0.97	3.83 ± 0.25 B
Listeria monocytogenes				
LP Hg lamp (254 nm)	1.56 ± 0.60	1.39 ± 0.35	0.99	5.01 ± 0.38 A
KrCl exilamp (222 nm)	0.79 ± 0.05	1.02 ± 0.04	0.99	3.84 ± 0.03 B
Salmonella Typhimurium				
LP Hg lamp (254 nm)	0.94 ± 0.17	1.16 ± 0.16	0.98	3.78 ± 0.00 A
KrCl exilamp (222 nm)	0.55 ± 0.09	0.97 ± 0.09	0.99	2.92 ± 0.08 B
Escherichia coli O157:H7				
LP Hg lamp (254 nm)	0.02 ± 0.01	0.35 ± 0.05	0.99	1.57 ± 0.29 A
KrCl exilamp (222 nm)	0.06 ± 0.03	0.48 ± 0.08	0.96	1.55 ± 0.22 A

SE, standard error, R^2, regression coefficient, SD, standard deviation. Values within each column for each pathogen followed by the same letter are not significantly different ($P > .05$).

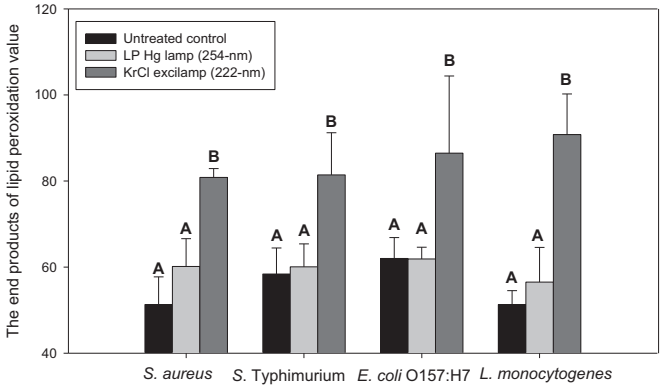

Fig. 2. The end products of lipid peroxidation values of *S. aureus*, *S.* Typhimurium, *E. coli* O157:H7 and *L. monocytogenes* from TBARS assay. Data represent an average of three independent experiments and the standard deviation shown by error bars. Different letters within the same pathogen cluster of treatments indicate significant differences ($P < .05$).

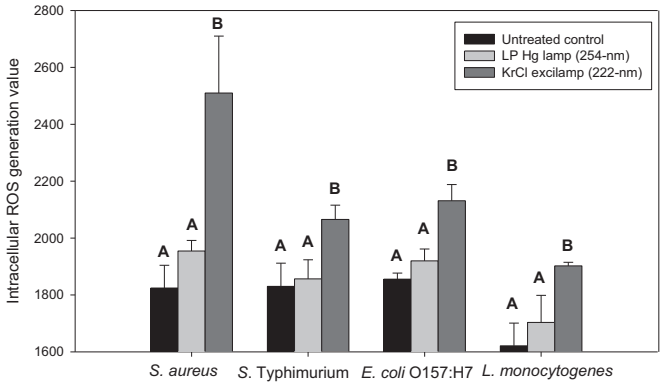

Fig. 3. Intracellular ROS generation values of *S. aureus*, *S.* Typhimurium, *E. coli* O157:H7 and *L. monocytogenes* from the ROS detection assay by CM-H_2DCFDA. Data represent an average of three independent experiments and the standard deviation shown by error bars. Different letters within the same pathogen cluster of treatments indicate significant differences ($P < .05$).

alongside that of a LP Hg lamp (Figs. 2, 3, and 4, Tables 2 and 3).

First, to examine cellular membrane damage, the degree of depolarization was measured. As shown in Table 2, there were no significant ($P > .05$) increases in depolarization value compared to untreated

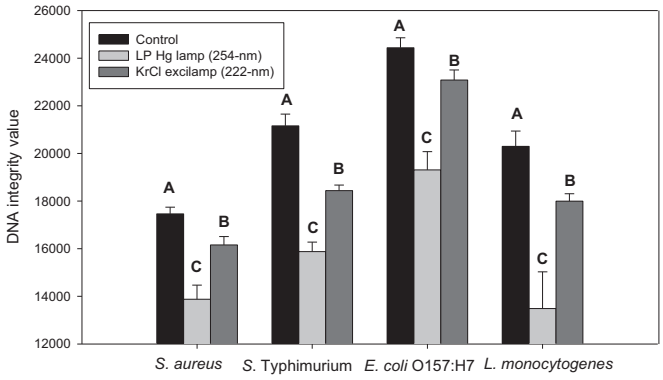

Fig. 4. DNA integrity values of *S. aureus*, *S.* Typhimurium, *E. coli* O157:H7 and *L. monocytogenes* from the DNA quantification assay by SYBR green I. Data represent an average of three independent experiments and the standard deviation shown by error bars. Different letters within the same pathogen cluster of treatments indicate significant differences ($P < .05$). (For interpretation of the references to colour in this figure legend, the reader is referred to the web version of this article.)

controls for all pathogens for the LP Hg lamp; indicating that LP Hg lamps do not induce depolarization of cell membranes. However, depolarization values were significantly decreased after KrCl excilamp treatment. Therefore, KrCl excilamp treatment induces membrane depolarization while the LP Hg lamp does not. Membrane potential plays an important role in cell physiological processes by generating the proton motive force which is closely involved in ATP generation, substance transport, and bacterial chemotaxis (Sträuber & Müller, 2010). Therefore, membrane potential reflects the viability of cells as well as membrane integrity. To ascertain the cause of loss of membrane potential, we verified the activity of respiratory chain dehydrogenase following UV treatment because this enzyme is closely involved in the electron transfer process from donor to acceptor and doing so can generate a trans-membraneous proton motive force (Anraku, 1988; Weiss, Friedrich, Hofhaus, & Preis, 1991). As shown in Table 3, there were no significant ($P > .05$) decreases of respiratory chain dehydrogenase activity value compared to untreated controls for LP Hg lamp treatment; that is, LP Hg lamp does not lead to loss of enzymatic activity of respiratory chain dehydrogenase. However, the KrCl excilamp caused loss of enzymatic activity of respiratory chain dehydrogenase because there were significantly ($P < .05$) decreased respiratory chain dehydrogenase activity values compared to untreated controls for all pathogens. Therefore, it was demonstrated that enzymatic activity is

Table 2
Depolarization values of *S. aureus*, *S.* Typhimurium, *E. coli* O157:H7 and *L. monocytogenes* from cell membrane potential assay by $DiBAC_4(3)$.

Value	Treatment	Microorganism			
		S. aureus	*S.* Typhimurium	*E. coli* O157:H7	*L. monocytogenes*
Depolarization value	Untreated control	562 ± 49 A	2844 ± 212 A	1603 ± 161 A	1240 ± 107 A
	LP Hg lamp (254 nm)	600 ± 66 A	3118 ± 160 A	1780 ± 206 A	1424 ± 147 A
	KrCl excilamp (222 nm)	765 ± 87 B	3984 ± 549 B	2237 ± 264 B	1956 ± 238 B

Values are means of three replications ± standard deviations.
Different letters within the same pathogen column indicate significant differences ($P < .05$).

Table 3
Respiratory chain dehydrogenase activity values of *S. aureus*, *S.* Typhimurium, *E. coli* O157:H7 and *L. monocytogenes* from enzymatic activity assay by INT.

Value	Treatment	Microorganism			
		S. aureus	*S.* Typhimurium	*E. coli* O157:H7	*L. monocytogenes*
Respiratory chain dehydrogenase activity value	Untreated control	2.06 ± 0.14 A	1.92 ± 0.09 A	4.96 ± 0.31 A	2.15 ± 0.21 A
	LP Hg lamp (254 nm)	2.04 ± 0.12 A	1.83 ± 0.07 A	4.87 ± 0.23 A	2.09 ± 0.25 A
	KrCl excilamp (222 nm)	1.44 ± 0.29 B	1.16 ± 0.33 B	4.34 ± 0.26 B	1.44 ± 0.24 B

Values are means of three replications ± standard deviations.
Different letters within the same pathogen column indicate significant differences ($P < .05$).

decreased only by KrCl excilamp treatment. Through this enzymatic assay, it is inferred that inactivation of key enzymes related to membrane potential is one cause of loss of membrane potential. This loss of enzymatic activity by KrCl excilamp treatment is in agreement with results of another study (Ha et al., 2017); they confirmed the denaturation of another intracellular enzyme (esterase) after KrCl excilamp treatment. Therefore, it can be thought that KrCl excilamp treatment effectively reduces enzyme activity which is essential to maintaining viability. Additionally, membrane damage can also occur in the form of physical destruction; for example, Ha et al. (2017) revealed the destruction of cell membranes caused by KrCl excilamp treatment by means of PI uptake assay. Such a permanent loss of membrane integrity makes it difficult for cells to maintain homeostasis, leading to cell death (Pagán & Mackey, 2000). Accordingly, it may be considered that not only respiratory enzyme inactivation but also destruction of cell membranes is linked to loss of membrane potential. To identify the cause of membrane destruction, we first assumed that cell membrane destruction may occur due to lipid peroxidation, a term that refers to the oxidative degradation of phospholipids, cholesterol, and other unsaturated lipids because lipid peroxidation also is linked to destruction of cell membranes (Girotti, 1990). Fig. 2 demonstrates that there were no significant ($P > .05$) increases of lipid peroxidation value following LP Hg lamp treatment while increasing lipid peroxidation value occurred following KrCl excilamp treatment for all pathogens. Therefore, TBARS assay reveals that lipid peroxidation occurred following KrCl excilamp treatment.

From these results, therefore, it is determined that the KrCl excilamp causes cell membrane damage by adversely affecting lipids and proteins. For a more an in-depth analysis of the results, however, there is a need to understand what initiates cell membrane damage and why the damage only occurs with KrCl excilamp treatment and not with the LP Hg lamp.

Regarding the origins of membrane damage, two different mechanisms are involved. First, there is direct absorption of UV radiation by cellular components, most notably lipids and proteins in the cellular membrane that can lead to photo-induced reactions (Costanzo, De Guidi, Giuffrida, Sortino, & Condorelli, 1995; Pattison & Davies, 2006). That is, there are direct photo-induced reactions of cell membranes and this is observed to disrupt cell membrane potential and permeability. Secondly, there is the possibility of photosensitized processes where direct absorbance by the cellular components (endogenous chromophores within the component) or exogenous photosensitization can produce an excited state or radicals as a result of photo-ionization (Gao, Xing, Li, & Zhang, 2008; Kramer & Muranyi, 2014; Pattison & Davies, 2006). It is well established that absorption of UV light by major chromophoric amino acids such as tryptophan (Typ), tyrosine (Tyr), phenylalanine (Phe), histidine (His) and cysteine (Cys) present in protein can lead to the generation of excited state species and radicals via photo-ionization (Bensasson, Land, & Truscott, 2013; Pattison & Davies, 2006). In other words, although direct photo-induced reactions are the initial event of UV-induced damage, they are not an end in themselves because UV absorption can also generate excited states or radicals as a result of photo-ionization which can give rise to secondary damage. To identify this, we measured the generation of ROS following both UV treatments. As shown in Fig. 3, intracellular ROS generation values of KrCl excilamp-treated cells increased significantly ($P < .05$) compared to untreated cells, while no significant ($P > .05$) increase of fluorescence values occurred after LP Hg treatment for all pathogens. In other words, there is generation of intracellular ROS caused by KrCl excilamp treatment but not by LP Hg treatment. Accordingly, it is inferred that UV light irradiated by the KrCl excilamp induces intracellular ROS generation and then adversely affects cell membrane integrity as a secondary form of damage.

With respect to damage induced only by KrCl excilamp (but not by LP Hg lamp) treatment, it can be understood due to the relative wavelength absorption property of materials. In the case of cellular membrane proteins, even though the absorption wavelength of amino acids varies depending on the type of amino acid, the maximum absorption wavelengths of major amino acids (Tyr, Typ, Phe, His, and Cys) are all under 240 nm (Bensasson et al., 2013). Furthermore, all proteins have an additional higher absorption from 180 to 230 nm because the absorption wavelength of the peptide backbone ranges from 180 to 230 nm (Marcus Clauss & Grotjohann, 2008; Kerwin & Remmele, 2007). In the case of lipid components of cell membranes, the result of UV absorption spectra of diacetylenic phospholipid and saturated phospholipid (Spector et al., 1996) indicates increasing absorption from 250 nm to a peak centered at 198 and 209 nm, respectively, and the absorption scale of diacetylenic phospholipid is 50 times that of saturated phospholipid. The spectral characteristic of saturated phospholipid is from the ester chromophore in the glycerol backbone of the lipid head group and that of the diacetylenic phospholipid is from the conjugated diacetylenes showing intense high UV absorption. Taken together, the characteristics of proteins and lipids which are major cellular components, both manifest a higher absorption at 222 nm

Table 4
Log reductions of *S. aureus*, *L. monocytogenes*, *S.* Typhimurium and *E. coli* O157:H7 suspended in PBS after treatment with a 254 nm LP lamp and 222 nm KrCl excilamp.

		Log reduction [Log_{10} (N0/N)][a] by treatment type and selection medium							
Treatment type	Treatment time (mJ/cm^2)	*S. aureus*		*L. monocytogenes*		*S.* Typhimurium		*E. coli* O157:H7	
		BPA	OV-BPA	OAB	OV-OAB	XLD	OV-XLD	SMAC	SPRAB
254 nm LP Hg lamp	0	0.00 ± 0.00 Aa	0.00 ± 0.00 Aa	0.00 ± 0.00 Aa	0.00 ± 0.00 Aa	0.00 ± 0.00 Aa	0.00 ± 0.00 Aa	0.00 ± 0.00 Aa	0.00 ± 0.00 Aa
	1	0.26 ± 0.09 Ba	0.21 ± 0.11 Ba	0.46 ± 0.27 Ba	0.52 ± 0.09 Ba	1.66 ± 0.05 Ba	1.21 ± 0.19 Bb	4.26 ± 0.28 Ba	3.87 ± 0.20 Ba
	2	1.27 ± 0.16 Ca	1.20 ± 0.18 Ca	1.22 ± 0.38 Ba	1.07 ± 0.37 Ba	2.29 ± 0.43 Ca	1.77 ± 0.51 Ba	5.56 ± 0.62 Ca	5.18 ± 0.32 Ca
	3	2.47 ± 0.44 Da	2.38 ± 0.28 Da	2.50 ± 0.64 Ca	2.35 ± 0.42 Ca	3.53 ± 0.37 Da	3.05 ± 0.49 Ca	6.25 ± 0.36 Da	5.60 ± 0.28 Da
	4	3.85 ± 0.08 Ea	3.84 ± 0.10 Ea	3.81 ± 0.64 Da	3.81 ± 0.32 Da	5.68 ± 0.37 Ea	4.95 ± 0.14 Db	6.85 ± 0.10 CDa	6.29 ± 0.04 Eb
	5	4.64 ± 0.20 Fa	4.65 ± 0.29 Fa	4.74 ± 0.66 Ea	4.50 ± 0.41 Ea	7.00 ± 0.16 Fa	6.15 ± 0.15 Eb	7.46 ± 0.10 Da	7.47 ± 0.07 Fa
	6	5.47 ± 0.49 Ga	5.60 ± 0.37 Ga	6.24 ± 0.12 Fa	5.76 ± 0.37 Fa		7.16 ± 0.23 F		
222 nm KrCl excilamp	0	0.00 ± 0.00 Aa	0.00 ± 0.00 Aa	0.00 ± 0.00 Aa	0.00 ± 0.00 Aa	0.00 ± 0.00 Aa	0.00 ± 0.00 Aa	0.00 ± 0.00 Aa	0.00 ± 0.00 Aa
	1	0.66 ± 0.06 Ba	0.74 ± 0.09 Ba	1.08 ± 0.20 Ba	1.13 ± 0.32 Ba	2.06 ± 0.46 Ba	2.05 ± 0.45 Ba	4.38 ± 0.46 Ba	3.91 ± 0.52 Ba
	2	1.96 ± 0.01 Ca	1.90 ± 0.14 Ca	2.40 ± 0.09 Ca	2.40 ± 0.19 Ca	3.37 ± 0.28 Ca	3.34 ± 0.37 Ca	5.82 ± 1.06 Ca	5.50 ± 0.62 Ca
	3	4.16 ± 0.53 Da	3.99 ± 0.33 Da	3.83 ± 0.19 Da	3.46 ± 0.13 Db	5.11 ± 0.19 Da	4.68 ± 0.14 Db	6.86 ± 0.10 Da	6.23 ± 0.21 Db
	4	5.37 ± 0.41 Ea	5.42 ± 0.45 Ea	5.53 ± 0.20 Ea	5.09 ± 0.20 Ea	7.00 ± 0.12 Ea	6.49 ± 0.18 Ea	7.46 ± 0.10 Ea	7.59 ± 0.08 Eb
	5	6.43 ± 0.43 Fa	6.39 ± 0.28 Fa	6.24 ± 0.12 Fa	6.50 ± 0.16 Fa		7.22 ± 0.15 F		
	6	7.09 ± 0.42 Ga	7.12 ± 0.13 Ga						

Different uppercase letters within the same column indicate significant differences ($P < .05$).
Different lowercase letters within the same row indicate significant differences ($P < .05$) for each pathogen.
BPA, Baird-Parker Agar; OV-BPA, overlay BPA on TSA; OAB, Oxford agar base with antimicrobial supplement; OV-OAB, overlay OAB agar on TSA; XLD, xylose lysine desoxycholate agar; OV-XLD, overlay XLD agar on TSA; SMAC, sorbitol MacConkey agar; SPRAB, phenol red agar base with 1% sorbitol.
[a] The values are means ± standard deviations from three replications.

emitted by the KrCl excilamp than at 254 nm emitted by the LP Hg lamp. Due to their higher absorption at 222 than at 254 nm, there are more occurrences of cell membrane damage due to direct photo-induced reactions as well as oxidative stress by ROS generated via photoionization in KrCl excilamp versus LP Hg lamp treatment. Even though UV irradiation (254 nm) emitted by the LP Hg lamp is absorbed less by proteins and lipids than that emitted by the KrCl excilamp, the LP Hg lamp also can affect lipids or proteins because its UV irradiation is absorbed as well. However, there was no occurrence of lipid or protein damage under the conditions of D_{5d} LP Hg lamp treatment used in our study. Additionally, it is assumed that lipid damage may increase if the degree of unsaturated fatty acids increased due to high UV absorption of conjugated double- or triple-bonds.

Simultaneously, DNA is considered as one of the most significant biological targets of UV-induced damage in bacteria because UV can affect crucial cellular processes such as DNA replication and transcription and compromise cellular viability and functional integrity and thus ultimately leads to cell death (Britt, 2004; Lindahl, 1993; Rastogi, Kumar, Tyagi, & Sinha, 2010). Consequently, the influence of UV treatment on DNA integrity was measured. As shown in Fig. 4, there was a significant ($P < .05$) decrease of DNA integrity values following both KrCl excilamp and LP Hg lamp treatments compared to the untreated control. However, the extent of DNA integrity value induced by the LP Hg lamp was significantly ($P < .05$) much lower than that of the KrCl excilamp. That is, there were occurrences of DNA damage resulting from both KrCl excilamp and LP Hg lamp treatment but DNA damage from the LP Hg lamp was higher than that of the KrCl excilamp. Generally, direct UVC (100–280 nm) absorption of DNA leads to the formation of cyclobutane pyrimidine dimers and (6–4) photoproducts which are of importance for the cytotoxic, mutagenic effect of UVC radiation (Cadet, Anselmino, Douki, & Voituriez, 1992; Evans et al., 1999; Kielbassa, Roza, & Epe, 1997). Furthermore, it has been well established that ROS generated by excited photosensitizers also induce damage as a form of oxidative DNA modification indirectly (Evans et al., 1999; Kielbassa et al., 1997; Zhang, Rosenstein, Wang, Lebwohl, & Wei, 1997). Evans et al. (1999) demonstrates that ROS ($^1O_2$) are involved in the induction of oxidative DNA damage by UVC (254 nm) radiation treatment. In contrast with this study, however, there was no induction of ROS by UV radiation at 254 nm treatment in our study. It may be surmised that there was not enough input of energy to generate ROS because samples were exposed to 254 nm UV radiation at a maximum dose of only 5.31 mJ/cm^2, while samples at this same wavelength were exposed to 100 mJ/cm^2 in the study of Evans et al. (1999). Therefore, it is concluded that DNA damage is attributed solely to direct UV (254 nm) absorption by DNA during 5-log reduction in our study. Additionally, our result that DNA damage by LP Hg lamp (254 nm) was greater than that of KrCl excilamp treatment may be related to the degree of UV radiation absorption. The UV absorption spectrum for DNA shows an absorbance band increasing at about 220 nm and peaking at 260 nm (Pattison & Davies, 2006; Taylor, 1994); thus, UV absorption by DNA at 254 nm is higher than that at 222 nm. Therefore, there was greater DNA damage following LP Hg lamp than KrCl excilamp treatment due to differences of UV absorption. Even though we observed less DNA damage by KrCl excilamp than by LP Hg lamp treatment, the 222 nm KrCl excilamp can cause DNA damage by inducing ROS generation and/or direct absorption affecting DNA integrity. Ubiquitous bacterial chromophores such as amino acids, which efficiently absorb 222 nm UV, can induce ROS formation and indirectly effect DNA damage.

It is important to consider sublethally injured cells after UV-C treatment with regard to food safety, as they can recover and regain normal pathogenicity under suitable conditions (Wu, 2008). Whereas sublethally injured cells are unable to recover after direct plating on selective media, they can resuscitate and be identified using the OV method (or SPRAB agar in the case of *E. coli* O157:H7). As shown in Table 4, overall, there were no significant ($P > .05$) differences between reduction levels determined by subjecting treated samples to cell recovery methods versus direct plating on selective media, but significant ($P < .05$) differences occurred at certain treatment doses, except for *S. aureus*, *L. monocytogenes* in the case of 254 nm LP lamp and KrCl exilamp. In other words, both treatments in general effectively controlled foodborne pathogens in PBS without causing sublethal injury, but sublethal injury occurred at some doses. When microorganisms undergo sublethal injury, many structural and functional cellular materials such as cell walls, cytoplasmic or inner membranes, ribosomes, DNA, RNA, and enzymes are affected and thus cellular changes occur (Ray, 1979, 1992). Therefore, based on this study's results, it can be inferred that sublethal injury by 254 nm LP lamp treatment was

mainly due to DNA damage, whereas sublethal injury following 222 nm KrCl excilamp treatment was due to membrane, enzyme, and DNA damage.

In conclusion, this research suggests that KrCl excilamps may be a potential substitute for LP Hg lamps due to their greater bactericidal effect against Gram-positive and Gram-negative pathogenic bacteria compared to LP Hg lamps. UV radiation can induce biological damage through two discrete ways: (i) direct absorption of UV radiation by cellular materials which can lead to photo-induced reactions, and (ii) secondary damage caused by oxidative products generated by photosensitized processes. The bactericidal mechanism of the KrCl excilamp is different from that of LP Hg lamps; this difference is related to the different cellular materials which absorb their emitting wavelengths. That is, the KrCl excilamp affects the cellular enzymes or membrane lipids because amino acids or phospholipids especially absorb UV radiation of 222 nm. Moreover, ubiquitous chromophores such as amino acids can generate ROS at this wavelength and thus even DNA, which does not absorb UV radiation at 222 nm very well, can be indirectly but significantly damaged by ROS. Therefore, it is considered that KrCl excilamp treatment simultaneously affects various cellular materials comprising multiple targets. Meanwhile, the LP Hg lamp solely affects DNA directly because only DNA among cellular materials is especially vulnerable to 254 nm UV radiation. These results further advance the findings of a previous study (Ha et al., 2017) analyzing the inactivation mechanisms of KrCl excilamps and underscore their potential usefulness. A detailed understanding of the inactivation mechanisms of this novel technology is important not only to identify the rate-limiting step during the inactivation process, but also to make it easier to interpret the presence or absence of any synergistic effect in combination application with other technologies and consequently help develop more effective inactivation strategies (Cho, Kim, Kim, Yoon, & Kim, 2010). Therefore, we expect to present this mechanism analysis as base line data for practical application or further research investigations involving KrCl excilamps.

Acknowledgments

This work was supported by Korea Institute of Planning and Evaluation for Technology in Food, Agriculture, Forestry (IPET) through Agriculture, Food and Rural Affairs Research Center Support Program, funded by Ministry of Agriculture, Food and Rural Affairs (MAFRA) (710012-03-1-HD220). This work was also supported by Korea Institute of Planning and Evaluation for Technology in Food, Agriculture, Forestry (IPET) through High Value-added Food Technology Development Program, funded by Ministry of Agriculture, Food and Rural Affairs (MAFRA) (117064-03-1-HD050).

References

Anraku, Y. (1988). Bacterial electron transport chains. *Annual Review of Biochemistry, 57*(1), 101–132.
Aoyagi, Y., Takeuchi, M., Yoshida, K., Kurouchi, M., Yasui, N., Kamiko, N., ... Nanishi, Y. (2011). Inactivation of bacterial viruses in water using deep ultraviolet semiconductor light-emitting diode. *Journal of Environmental Engineering, 137*(12), 1215–1218.
Beck, S. E., Wright, H. B., Hargy, T. M., Larason, T. C., & Linden, K. G. (2015). Action spectra for validation of pathogen disinfection in medium-pressure ultraviolet (UV) systems. *Water Research, 70*, 27–37.
Bensasson, R., Land, E., & Truscott, T. (2013). *Flash photolysis and pulse radiolysis: Contributions to the chemistry of biology and medicine.* Elsevier.
Berk, Z. (2008). *Food process engineering and technology.* Academic Press.
van Boekel, M. A. (2002). On the use of the Weibull model to describe thermal inactivation of microbial vegetative cells. *International Journal of Food Microbiology, 74*(1), 139–159.
Britt, A. B. (2004). Repair of DNA damage induced by solar UV. *Photosynthesis Research, 81*(2), 105–112.
Caillier, B., Caiut, J. M. A., Muja, C., Demoucron, J., Mauricot, R., Dexpert-Ghys, J., & Guillot, P. (2015). Decontamination efficiency of a DBD lamp containing an UV–C emitting phosphor. *Photochemistry and Photobiology, 91*(3), 526–532.
Cadet, J., Anselmino, C., Douki, T., & Voituriez, L. (1992). New trends in photobiology: Photochemistry of nucleic acids in cells. *Journal of Photochemistry and Photobiology B: Biology, 15*(4), 277–298.
Chatterley, C., & Linden, K. (2010). Demonstration and evaluation of germicidal UV-LEDs for point-of-use water disinfection. *Journal of Water and Health, 8*(3), 479–486.
Chevremont, A.-C., Boudenne, J.-L., Coulomb, B., & Farnet, A.-M. (2013a). Fate of carbamazepine and anthracene in soils watered with UV-LED treated wastewaters. *Water Research, 47*(17), 6574–6584.
Chevremont, A.-C., Boudenne, J.-L., Coulomb, B., & Farnet, A.-M. (2013b). Impact of watering with UV-LED-treated wastewater on microbial and physico-chemical parameters of soil. *Water Research, 47*(6), 1971–1982.
Cho, M., Kim, J., Kim, J. Y., Yoon, J., & Kim, J.-H. (2010). Mechanisms of Escherichia coli inactivation by several disinfectants. *Water Research, 44*(11), 3410–3418.
Close, J., Ip, J., & Lam, K. (2006). Water recycling with PV-powered UV-LED disinfection. *Renewable Energy, 31*(11), 1657–1664.
Costanzo, L., De Guidi, G., Giuffrida, S., Sortino, S., & Condorelli, G. (1995). Antioxidant effect of inorganic ions on UVC and UVB induced lipid peroxidation. *Journal of Inorganic Biochemistry, 59*(1), 1–13.
Clauss, M., & Grotjohann, N. (2008). Effective Photoinactivation of alpha-amylase, catalase and urease at 222 nm emitted by an KrCl-Excimer lamp. *CLEAN–Soil, Air, Water, 36*(9), 754–759.
Clauss, M., Springorum, A., & Hartung, J. (2009). Ultraviolet disinfection with 222 nm wavelength-new options to inactivate UV-resistant pathogens. *Paper presented at the Sustainable animal husbandry: Prevention is better than cure, Volume 2. Proceedings of the 14th International Congress of the International Society for Animal Hygiene (ISAH), Vechta, Germany, 19th to 23rd July 2009*.
Dotson, A. D., Rodriguez, C. E., & Linden, K. G. (2012). UV disinfection implementation status in US water treatment plants. *Journal of American Water Works Association, 104*(5).
Dragan, A., Pavlovic, R., McGivney, J., Casas-Finet, J., Bishop, E., Strouse, R., ... Geddes, C. (2012). SYBR green I: Fluorescence properties and interaction with DNA. *Journal of Fluorescence, 22*(4), 1189–1199.
Evans, M. D., Cooke, M. S., Podmore, I. D., Zheng, Q., Herbert, K. E., & Lunec, J. (1999). Discrepancies in the measurement of UVC-induced 8-oxo-2′-deoxyguanosine: Implications for the analysis of oxidative DNA damage. *Biochemical and Biophysical Research Communications, 259*(2), 374–378.
Fan, X., Huang, R., & Chen, H. (2017). Application of ultraviolet C technology for surface decontamination of fresh produce. *Trends in Food Science & Technology, 60*, 9–19.
Gao, C., Xing, D., Li, L., & Zhang, L. (2008). Implication of reactive oxygen species and mitochondrial dysfunction in the early stages of plant programmed cell death induced by ultraviolet-C overexposure. *Planta, 227*(4), 755–767.
Gayán, E., Serrano, M., Pagán, R., Álvarez, I., & Condón, S. (2015). Environmental and biological factors influencing the UV-C resistance of Listeria monocytogenes. *Food Microbiology, 46*, 246–253.
Geeraerd, A., Valdramidis, V., & Van Impe, J. (2005). GInaFiT, a freeware tool to assess non-log-linear microbial survivor curves. *International Journal of Food Microbiology, 102*(1), 95–105.
Girotti, A. W. (1990). Photodynamic lipid peroxidation in biological systems. *Photochemistry and Photobiology, 51*(4), 497–509.
Ha, J.-W., Lee, J.-I., & Kang, D.-H. (2017). Application of a 222-nm krypton-chlorine excilamp to control foodborne pathogens on sliced cheese surfaces and characterization of the bactericidal mechanisms. *International Journal of Food Microbiology, 243*, 96–102.
Han, L., Patil, S., Boehm, D., Milosavljević, V., Cullen, P., & Bourke, P. (2016). Mechanisms of inactivation by high-voltage atmospheric cold plasma differ for *Escherichia coli* and *Staphylococcus aureus*. *Applied and Environmental Microbiology, 82*(2), 450–458.
Harm, W. (1980). *Biological effects of ultraviolet radiation*.
Joshi, S. G., Cooper, M., Yost, A., Paff, M., Ercan, U. K., Fridman, G., & Brooks, A. D. (2011). Nonthermal dielectric-barrier discharge plasma-induced inactivation involves oxidative DNA damage and membrane lipid peroxidation in Escherichia coli. *Antimicrobial Agents and Chemotherapy, 55*(3), 1053–1062.
Kerwin, B. A., & Remmele, R. L. (2007). Protect from light: Photodegradation and protein biologics. *Journal of Pharmaceutical Sciences, 96*(6), 1468–1479.
Kielbassa, C., Roza, L., & Epe, B. (1997). Wavelength dependence of oxidative DNA damage induced by UV and visible light. *Carcinogenesis, 18*(4), 811–816.
Kramer, B., & Muranyi, P. (2014). Effect of pulsed light on structural and physiological properties of *Listeria innocua* and *Escherichia coli*. *Journal of Applied Microbiology, 116*(3), 596–611.
Kalyanaraman, B., Darley-Usmar, V., Davies, K. J., Dennery, P. A., Forman, H. J., Grisham, M. B., & Ischiropoulos, H. (2012). Measuring reactive oxygen and nitrogen species with fluorescent probes: Challenges and limitations. *Free Radical Biology and Medicine, 52*(1), 1–6.
Lee, S.-Y., & Kang, D.-H. (2001). Suitability of overlay method for recovery of heat-injured *Listeria monocytogenes* and *Salmonella typhimurium*. *Food Science and Biotechnology, 10*(3), 323–326.
Lindahl, T. (1993). Instability and decay of the primary structure of DNA. *Nature, 362*(6422), 709–715.
Li, W.-R., Xie, X.-B., Shi, Q.-S., Zeng, H.-Y., You-Sheng, O.-Y., & Chen, Y.-B. (2010). Antibacterial activity and mechanism of silver nanoparticles on *Escherichia coli*. *Applied Microbiology and Biotechnology, 85*(4), 1115–1122.
Liao, X., Liu, D., Xiang, Q., Ahn, J., Chen, S., Ye, X., & Ding, T. (2017). Inactivation mechanisms of non-thermal plasma on microbes: A review. *Food Control, 75*, 83–91.
Lubello, C., Gori, R., Nicese, F. P., & Ferrini, F. (2004). Municipal-treated wastewater reuse for plant nurseries irrigation. *Water Research, 38*(12), 2939–2947.
Matafonova, G., & Batoev, V. (2012). Recent progress on application of UV excilamps for degradation of organic pollutants and microbial inactivation. *Chemosphere, 89*(6), 637–647.

Matafonova, G., Batoev, V., Astakhova, S., Gomez, M., & Christofi, N. (2008). Efficiency of KrCl excilamp (222 nm) for inactivation of bacteria in suspension. *Letters in Applied Microbiology, 47*(6), 508–513.
Mikš-Krajnik, M., Yuk, H.-G., Kumar, A., Yang, Y., Zheng, Q., Kim, M.-J., ... Pang, X. (2015). Ensuring food security through enhancing microbiological food safety. *Cosmos, 11*(01), 69–97.
Mir, S. A., Shah, M. A., & Mir, M. M. (2016). Understanding the role of plasma technology in food industry. *Food and Bioprocess Technology, 9*(5), 734–750.
Mori, M., Hamamoto, A., Takahashi, A., Nakano, M., Wakikawa, N., Tachibana, S., ... Kinouchi, Y. (2007). Development of a new water sterilization device with a 365 nm UV-LED. *Medical & Biological Engineering & Computing, 45*(12), 1237–1241.
Negre-Salvayre, A., Augé, N., Duval, C., Robbesyn, F., Thiers, J.-C., Nazzal, D., ... Salvayre, R. (2002). [5] Detection of intracellular reactive oxygen species in cultured cells using fluorescent probes. *Methods in Enzymology, 352*, 62–71.
Orlowska, M., Koutchma, T., Kostrzynska, M., & Tang, J. (2015). Surrogate organisms for pathogenic O157: H7 and non-O157 Escherichia coli strains for apple juice treatments by UV-C light at three monochromatic wavelengths. *Food Control, 47*, 647–655.
Pagán, R., & Mackey, B. (2000). Relationship between membrane damage and cell death in pressure-treated Escherichia coli cells: Differences between exponential-and stationary-phase cells and variation among strains. *Applied and Environmental Microbiology, 66*(7), 2829–2834.
Pattison, D. I., & Davies, M. J. (2006). Actions of ultraviolet light on cellular structures. *Cancer: Cell structures, carcinogens and genomic instability* (pp. 131–157). Springer.
Rahmani, B., Hafsa, C., Kacem, M., Harche, M. K., Bhosle, S., Aubes, M., & Zissis, G. (2010). Photoinactivation of the Escherichia coli by the pulsed dielectric barrier discharge excilamp krypton chlorine emitted at 222 nm. *IEEE Transactions on Plasma Science, 38*(4), 953–956.
Rastogi, R. P., Kumar, A., Tyagi, M. B., & Sinha, R. P. (2010). Molecular mechanisms of ultraviolet radiation-induced DNA damage and repair. *Journal of Nucleic Acids, 2010*.
Ray, B. (1979). Methods to detect stressed microorganisms. *Journal of Food Protection, 42*(4), 346–355.
Ray, B. (1992). Sublethal injury, bacteriocins and food microbiology. *ASM News, 59*, 285.
Rhee, M.-S., Lee, S.-Y., Hillers, V. N., McCURDY, S. M., & Kang, D.-H. (2003). Evaluation of consumer-style cooking methods for reduction of *Escherichia coli* O157: H7 in ground beef. *Journal of Food Protection, 66*(6), 1030–1034.
Sivapalasingam, S., Friedman, C. R., Cohen, L., & Tauxe, R. V. (2004). Fresh produce: A growing cause of outbreaks of foodborne illness in the United States, 1973 through 1997. *Journal of Food Protection, 67*(10), 2342–2353.
Sosnin, E. A. (2007). Excimer lamps and based on them a new family of ultraviolet radiation sources. *Light Engineering,* 15(1), 49–57.
Spector, M. S., Easwaran, K. R., Jyothi, G., Selinger, J. V., Singh, A., & Schnur, J. M. (1996). Chiral molecular self-assembly of phospholipid tubules: A circular dichroism study. *Proceedings of the National Academy of Sciences, 93*(23), 12943–12946.
Sträuber, H., & Müller, S. (2010). Viability states of bacteria—Specific mechanisms of selected probes. *Cytometry Part A, 77*(7), 623–634.
Taylor, J. S. (1994). Unraveling the molecular pathway from sunlight to skin cancer. *Accounts of Chemical Research, 27*(3), 76–82.
Wang, D., Oppenländer, T., El-Din, M. G., & Bolton, J. R. (2010). Comparison of the disinfection effects of vacuum-UV (VUV) and UV light on Bacillus subtilis spores in aqueous suspensions at 172, 222 and 254 nm. *Photochemistry and Photobiology, 86*(1), 176–181.
Weiss, H., Friedrich, T., Hofhaus, G., & Preis, D. (1991). The respiratory-chain NADH dehydrogenase (complex I) of mitochondria. *European Journal of Biochemistry, 197*(3), 563–576.
Wojtala, A., Bonora, M., Malinska, D., Pinton, P., Duszynski, J., & Wieckowski, M. R. (2014). Methods to monitor ROS production by fluorescence microscopy and fluorometry. *Methods in Enzymology, 542*, 243–262.
Wu, V. (2008). A review of microbial injury and recovery methods in food. *Food Microbiology, 25*(6), 735–744.
Yin, F., Zhu, Y., Koutchma, T., & Gong, J. (2015). Inactivation and potential reactivation of pathogenic Escherichia coli O157: H7 in apple juice following ultraviolet light exposure at three monochromatic wavelengths. *Food Microbiology, 46*, 329–335.
Zhang, X., Rosenstein, B. S., Wang, Y., Lebwohl, M., & Wei, H. (1997). Identification of possible reactive oxygen species involved in ultraviolet radiation-induced oxidative DNA damage. *Free Radical Biology and Medicine, 23*(7), 980–985.
Ziuzina, D., Patil, S., Cullen, P. J., Keener, K., & Bourke, P. (2014). Atmospheric cold plasma inactivation of *Escherichia coli*, *Salmonella enterica serovar Typhimurium* and *Listeria monocytogenes* inoculated on fresh produce. *Food Microbiology, 42*, 109–116.